

The Linear Sizes of Quasars and Radio Galaxies in the Unified Scheme

Gopal-Krishna and V.K. Kulkarni

*National Centre for Radio Astrophysics, Tata Institute of Fundamental Research,
Poona University Campus, Post Bag. No. 3, Pune 411007, India
e-mail: krishna(vasant)@gmrt.ernet.in*

and Paul J. Wiita

*Department of Physics & Astronomy, Georgia State University, Atlanta, GA 30303-3083
e-mail: wiita@chara.gsu.edu*

ABSTRACT

A key argument in favor of orientation based unification schemes is the finding that among the most powerful 3CRR radio sources the (apparent) median linear size of quasars is smaller than that of radio galaxies, which supports the idea that quasars are a subset of radio galaxies, distinguished by being viewed at smaller angles to the line of sight. Recent measurements of radio sizes for a few other low frequency samples are, however, not in accord with this trend, leading to the claim that orientation may not be the main difference between radio galaxies and quasars. We point out that this “inconsistency” can be removed by making allowance for the temporal evolution of sources in both size and luminosity, as inferred from independent observations. This approach can also readily explain the other claimed “major discrepancy” with the unified scheme, namely, the difference between the radio luminosity–size correlations for quasars and radio galaxies.

Subject headings: galaxies: active — galaxies: jets — galaxies: quasars: general — radio continuum: galaxies

Accepted by ASTROPHYSICAL JOURNAL LETTERS on 13 March 1996

1. Introduction

According to a widely discussed unified scheme for powerful F-R II extragalactic radio sources (with luminosities above $\sim 10^{25.5}$ W Hz $^{-1}$ at 1 GHz, where we take $H_0 = 50$ km s $^{-1}$ Mpc $^{-1}$ and $q_0 = 0.5$ throughout this *Letter*), narrow-line radio galaxies (RGs) are identified as quasars (QSRs), or even blazars, whenever their principal axis happens to be oriented within a certain critical angle, ψ , from the line-of-sight (for recent reviews, see Antonucci 1993; Urry & Padovani 1995; Gopal-Krishna 1995, 1996). In this model, the parsec-scale nuclear core of such sources, consisting of a compact central engine ejecting relativistic jets of non-thermal continuum emission, and a broad line region (BLR), is believed to be surrounded by a dusty torus. In the case of RGs, the torus is believed to obscure the core in the visible through soft X-ray bands, so that the BLR is not directly visible. Strong evidence for such tori comes from the detection of the BLR in the (scattered) polarized light (e.g., Antonucci & Miller 1985; Cimatti et al. 1993; Draper, Scarrott & Tadhunter 1993). Various evidences for the relativistic beaming aspect of this picture include: extremely rapid variability of blazars over all bands; apparent superluminal motion in the bright radio cores; larger ratios of core to total radio emission, f_c , in QSRs than in RGs; correlation of f_c with the polarized optical nuclear continuum and its anti-correlations with apparent radio linear size, the symmetry of core-to-lobe separations, and the equivalent width of the [O II] $\lambda\lambda 3727$ line (Urry & Padovani 1995; Gopal-Krishna 1995, and references therein). The unified scheme is further supported by the analysis of the radio luminosity functions of the postulated parent and aligned populations (Padovani & Urry 1992).

One of the cornerstones of the orientation-based paradigm for powerful radio sources has been the observation that in the low-frequency 3CRR sample (Laing, Riley, & Longair 1983), where the axes of the sources should be randomly oriented, the median linear extent, ℓ , of the extended radio emission from QSRs *appears* significantly smaller ($\lesssim 50\%$ for redshifts $z > 0.5$) than that of RGs (Barthel 1989). However, the lack of such a behavior in the same sample at $z < 0.5$ (Kapahi 1990; Singal 1993a), bolstered by similar trends reported recently for a few other low-frequency samples a few times deeper in flux density than the 3CRR, has evoked serious doubts about

the unified scheme (Singal 1995, 1996; Kapahi et al. 1995). Here we show that this apparently irrefutable inconsistency with the data can be resolved quantitatively by taking into account the available strong independent evidence for temporal evolution in both the sizes and luminosities of extragalactic double radio sources.

2. Temporal and Luminosity Dependences of Radio Source Properties

Powerful radio sources are generally accepted to have rather limited lifetimes; these are typically estimated to be of the order of 10^7 yr, using the measured spatial gradients of spectral index across their radio lobes (e.g., Alexander & Leahy 1987; Liu, Pooley & Riley 1992). Although any particular “spectral age” determination is uncertain, and probably somewhat of an underestimate because of the complications arising from field inhomogeneities (Siah & Wiita 1990; Eilek 1996), inverse Compton losses of electron energy to the microwave background radiation (Wiita & Gopal-Krishna 1990), and backflow from the jets into the radio lobes (Liu et al. 1992; Scheuer 1995), significant centimeter wave emission persisting for times in excess of 10^8 yr is unlikely. During this active phase a double radio source grows in size through a hot circumgalactic medium at a speed V which depends weakly on both the radio luminosity, P ($V \propto P^\alpha$, $\alpha \simeq 0.3$) (Alexander & Leahy 1987; Liu et al. 1992) and time ($V \propto t^\beta$, $\beta \simeq -0.25$ to 0) (Gopal-Krishna & Wiita 1987, 1991; Fanti et al. 1996). Further, recent studies (Readhead 1995; Fanti et al. 1996), combining complete samples of powerful radio sources in different ranges of linear size, strongly suggest that the growth of a source from a few kpc to a few hundred kpc during the source lifetime is accompanied by typically an order-of-magnitude decrease in P (largely due to expansion losses), after which the nuclear activity subsides rapidly (Rees 1994). Thus, we shall take $T = 10^7$ yr as the characteristic e-folding time for the radio luminosity decay, and we approximate $P \propto \exp(-t/T)$, after a short-lived initial brightening phase during which the source turns on to a level related to the power of its jets. While, admittedly, neither fully constrained nor unique, this empirically supported characterization of luminosity evolution of individual sources appears to give a reasonable account of the temporal behavior of powerful extragalactic radio sources.

A key element (Antonucci & Miller 1985; Barthel 1989; Lawrence 1991) of the unified picture is the critical angle ψ , which separates the sources classified as narrow-line objects (RGs) from those called broad-line objects (QSRs). Assuming that all powerful radio sources are intrinsically similar, this angle is readily determined from the fraction, f_q , of sources identified as QSRs in a volume-limited sample of sources, if the sample is unbiased in orientation. (Alternative possibilities, such as the assumption that a subset of RGs whose optical spectra show only weak narrow-line emission would not exhibit broad lines from any viewing direction [e.g., Laing et al. 1994], exist but will not be considered further here, as we are interested in examining whether the simplest extensions of the unification scheme can be reconciled with the data.) In practice, such unbiased samples are selected at meter wavelengths, where the emission is dominated by radio lobes presumed to be radiating isotropically. Physically, ψ is identified with the half angle of the polar openings of the dusty obscuring torus surrounding the active galactic nucleus (e.g., Antonucci & Miller 1985; Antonucci 1993; Jaffe et al. 1993). Although earlier investigations (Kapahi 1990; Lawrence 1991; Singal 1993a) of the 3CRR sample suggested a systematic increase in ψ with P (or, z), this requirement was found to be less compelling in some recent studies (Laing et al. 1994; Saikia & Kulkarni 1994) of the same 3CRR sample. Nonetheless, comparisons of f_q 's found for the 3CRR and three other low-frequency complete samples which are selected at 408 MHz, have an expected $z(\text{median}) \sim 0.6$ (Condon 1993), and are roughly an order-of-magnitude deeper in flux density than the 3CRR sample, distinctly indicate a steady increase in ψ with P (Gopal-Krishna 1995; Singal 1995, 1996). Thus, beginning at large values of $\sim 50^\circ$ – 60° for the most luminous radio sources (namely, the 3CRR sources at $z > 1$), ψ appears to shrink gradually to 20° to 30° for sources in the samples selected at 408 MHz which are likely to be two orders-of-magnitude less luminous, on average (Gopal-Krishna 1995; Singal 1995, 1996). Note that we consider the dependence of ψ to be primarily on (initial) P instead of z , firstly because it is expected on theoretical grounds (see below), and secondly because such a dependence has also been inferred for optically selected active galactic nuclei (Falcke, Gopal-Krishna, & Biermann 1995, and references therein).

One likely theoretical explanation for the variation in torus opening angle involves the action of ener-

getic nuclear photons on the dust particles within the torus, so that more powerful central engines may be expected to have larger values of ψ (Netzer & Laor 1993; Königl & Kartje 1994). Note that for a given source, ψ need not decrease monotonically with time, as the secular decay of its radio luminosity (see above) can be expected to arise primarily from expansion losses (Scheuer 1974; Gopal-Krishna & Wiita 1991), rather than from a decline in the intrinsic jet power. The diminishing of the radio lobe pressure due to the expansion would also lead to a lowering of the optical output of the narrow-line emitting filaments within and around the lobe, thus explaining the correlation of the radio luminosity P with the narrow [O III] line emission, established by Baum & Heckman (1989) and Rawlings & Saunders (1991). The possibility exists, on the other hand, that ψ may increase with time, due to a steady rise in the mass of the central engine. The greater gravitational dominance of a more massive black hole over the surrounding stellar core is expected to push outward the inner edge of the molecular torus, due to a shift in the region where reduced differential rotation allows a piling-up of the accreted gas (Yi, Field, & Blackman 1994). Such a circumstance would facilitate our explanation for the apparent excess of the QSR radio sizes vis-à-vis RGs (see below).

3. The Model

In light of the above observations and discussion, we adopt the following simple relations to broadly represent the actual dependences for radio luminosity, critical angle, and physical (deprojected) size, respectively:

$$P(t) = P_0 \exp(-t/T), \quad \text{where } T = 10^7 \text{ yr}; \quad (1)$$

$$\psi(P_0) = a \log_{10}(P_0/10^{26} \text{ W Hz}^{-1}), \quad (2)$$

where $0.2 \text{ radian} \leq \psi \leq \psi_{\max} \simeq 1.0 \text{ radian}$;

$$L(P_0, t) \propto P_0^{b_1} t^{b_2}; \quad (3)$$

where a , b_1 and b_2 are constants (input parameters to the model) whose characteristic values can be approximated from the empirical estimates for f_q , α , and β mentioned above.

We can now compute the RG-to-QSR median linear size ratio, R , for a temporally evolving population of sources. Consider a radio luminosity, P ,

which is below the value for the most powerful radio sources created (P_{max}). At any particular time, the sources *observed* at the luminosity level P would include not just the young (hence small) sources freshly created with that level of luminosity, but also the aging sources that were born with higher luminosities in the past, but have since then faded down to P , and concurrently expanded to larger sizes. Since these older expanded radio sources with larger ℓ would have a higher QSR fraction (f_q) arising from their higher initial P_0 (and correspondingly larger ψ), the median radio size of QSRs found in intermediate luminosity samples with P substantially below P_{max} may well approach, or even exceed, that of RGs. This could possibly be the explanation for the reported radio size “anomaly” mentioned above (Gopal-Krishna 1995), which is claimed (Singal 1993a, 1995; Kapahi et al. 1995) to rule out the orientation based unified scheme.

To explore this proposal quantitatively, let us assume that a certain number of sources is “injected” continuously at a fixed rate (arbitrarily set to 100 per unit time) within a unit volume of space, with radio luminosities distributed as

$$N(P_0) \propto P_0^{-\Gamma}, \quad \text{for } P_0 \text{ up to } P_{max}. \quad (4)$$

Our simple model parameterized by Eqns. (1–4) can now be used to numerically predict the quasar fraction, f_q at a given P , as well as the corresponding ratio, R , of the median projected radio sizes of RGs and QSRs. To do this we first need to derive the distribution function of ages of sources of a given current luminosity P . To do so we start from the full distribution function of P and t , which is

$$\rho(P, t) = KP^{-\Gamma} \exp[-(\Gamma - 1)t/T]. \quad (5)$$

From this we derive the (normalized) distribution function of t for a given P to be

$$\Phi(t|P = P) = \frac{(\Gamma - 1)T^{-1} \exp[-(\Gamma - 1)t/T]}{[1 - (P/P_{0,max})^{\Gamma-1}]. \quad (6)}$$

We then generate a large number of sources, the ages of which follow this distribution. For each source we take its age, t_i , and its orientation angle from the line-of-sight, θ_i (randomly selected from 0 to $\pi/2$), yielding its $P_{0,i}$ (Eqn. 1) and ψ_i (Eqn. 2). If $\theta_i < \psi_i$ then the object is counted as a quasar, otherwise it is counted as a galaxy. We then obtain its linear size, L (Eqn. 3), and projected linear size, ℓ . By repeating

this procedure many times, we compute the median projected linear size for RGs and for QSRs (yielding R), as well as f_q , for the adopted value of P .

In Fig. 1 our simple model is confronted with the observations by plotting the combinations of f_q and R computed as above for different values of P , taking some characteristic values for the input parameters based on the above discussion and using additional observations to set $\Gamma \approx 2$ in Eqn. 6 (see Dunlop & Peacock 1990). In Eqn. 4, P_{max} , has been set equal to 10^{29}W Hz^{-1} at 1 GHz, characteristic of the most luminous radio sources. The runs of the computed values of f_q and R are shown by three curves, each covering a two orders-of-magnitude range in P . Approximately the same range is spanned by the data points, which are reproduced from Singal (1995), and correspond to subsets of the 3CRR, 1-Jy and B3 samples. Note that although redshifts for the B3 subset are not fully known, its median flux density of ~ 1 Jy at 408 MHz suggests (Condon 1993) a $z(\text{median}) \sim 0.6$, making it roughly two orders-of-magnitude less luminous, on average, than the most luminous 3CRR subset ($z \geq 1$) shown by the rightmost data point in Fig. 1. We further note that (in the absence of complete redshift information) although the size ratios given in Singal (1995; also, Fig. 1) actually refer to angular sizes, they are not likely to differ significantly from the linear size ratios, as most of the sources involved lie at $z \geq 0.5$ where the linear-to-angular conversion is relatively insensitive to z (see also Table 1 in Singal 1993a). Moreover, a similar drop in the value of R to around unity near $S_{408} \sim 1$ Jy has been inferred (Kapahi et al. 1995) from the linear sizes of the Molonglo QSRs and 3CRR RGs.

As highlighted by Singal (1995, 1996), the data points provide a poor match to the prediction of the orientation-based unified scheme (shown by the curve “U” in Fig. 1) for any single value of ψ ; even if ψ were allowed to vary, the predicted trend runs counter to the disposition of the data points. It is seen, however, that once an allowance is made for the (inevitable) temporal evolution broadly characterized by our simple, empirically supported model, the predicted f_q – R profiles for the unified scheme are found to match the data points quite well (Fig. 1).

An interesting implication of the present model is that except in the meter wavelength samples selected at the highest luminosities, quasars would be systematically *older* (and physically larger) than RGs. This is opposite to the situation envisioned in some alter-

native unification schemes (e.g., Hutchings, Price, & Gower 1988).

Finally, a cautionary remark, motivated by our implicit assumption that broad and narrow-line objects can be distinguished at all luminosities and redshifts. This assumption may not be valid at lower luminosities where any broad component underlying a narrow spectral feature may be increasingly hard to detect, leading to an underestimate of f_q (and, therefore, ψ). The significance of this potential bias cannot be quantified using the currently available data, though it is unlikely to be a major effect for the relatively luminous objects being considered here.

4. Conclusions

We emphasize that the temporal evolution incorporated here into the orientational unified scheme is exceedingly simple and expressed in terms of just a few parameters, all of which are constrained by observations. Since this evolutionary scenario is inspired by observations and elementary theoretical considerations, the neglect of this factor in the past attempts to verify the unified scheme was a major shortcoming. Consequently, the claimed “mismatch” with the radio size data (Singal 1993a, 1995, 1996; Kapahi et al. 1995) should not mandate dismissal of the paramount role assigned to orientation effects in the unified scheme.

The present explanation for the decreasing RG-to-QSR size ratio, R , towards lower radio luminosities also provides an explanation for an *equivalent* observational result according to which QSRs and RGs exhibit different ℓ - P correlations. Several authors have pointed out that the empirically derived positive ℓ - P dependence for RGs ($\ell \propto P^x$, $x \simeq +0.3$), contrasts with practically no ℓ - P dependence found for QSRs ($x \simeq 0$), and have argued that this “puzzling” result effectively rules out the unified scheme (Chyzy & Zieba 1993; Singal 1993a,b, 1995, 1996; Kapahi et al. 1995). However, this difference too, can be readily understood in our picture. The values of x corresponding to the three computed model curves shown in Fig. 1 are $+0.24 \pm 0.07$ for RGs and 0.09 ± 0.08 for QSRs, as deduced from the linear fits to the computed median sizes at different radio luminosities for the three sets of input parameters; for each fit the slope x is found to be greater for RGs than for QSRs. As a refinement to the present analysis, the use of full linear size distributions (rather than the median

values) would be a useful step.

In summary, we conclude that the linear size measurements of radio galaxies and quasars reported up to this point do not violate the basic tenet of the unified scheme, viz, that radio galaxies are oriented closer to the sky plane than are quasars.

We thank the anonymous referee for suggestions which led to improvements in the presentation. This work was supported in part by NSF grant AST-9102106, NASA grant NAG 5-3098, and Chancellor’s Initiative Funds at Georgia State University.

REFERENCES

Alexander, P. & Leahy, J.P. 1987, MNRAS, 225, 1
 Antonucci, R. 1993, ARA&A, 31, 473
 Antonucci, R.R.J., & Miller, J.S. 1985, ApJ, 297, 621
 Barthel, P.D. 1989, ApJ, 336, 606
 Baum, S.A., & Heckman, T. 1989, ApJ, 336, 702
 Chyzy, K.T., & Zieba, S. 1993, A&A, 267, L27
 Cimatti, A., de Serego Alighieri, S., Fosbury, R.A.E., Salvati, M., & Taylor, D. 1993, MNRAS, 264, 421
 Condon, J. 1993, in Sky Surveys: Protostars to Protogalaxies (ASP Conf. Ser. 43), ed. B.T. Soifer (San Francisco, ASP), 87
 Draper, P.W., Scarrott, S.M., & Tadhunter, C.N. 1993, MNRAS, 262, 1029
 Dunlop, J.S., & Peacock, J.A. 1990, MNRAS, 247, 19
 Eilek, J.A. 1996, in Energy Transport in Radio Galaxies & Quasars (ASP Conf. Ser.), eds. P. Hardee, A. Bridle, & A. Zensus (San Francisco, ASP), in press
 Falcke, H., Gopal-Krishna, & Biermann, P. 1995, A&A, 298, 395
 Fanti, C., Fanti, R., Dallacasa, D., Schilizzi, R.T., Spencer, R.E., & Stanghellini, C. 1996, A&A, in press
 Gopal-Krishna. 1995, Proc. Nat. Acad. Sci., 92, 11399
 _____. 1996, Proc. IAU Symposium No. 175 (Extragalactic Radio Sources), eds. C. Fanti & R.D. Ekers (Dordrecht, Kluwer), in press
 Gopal-Krishna & Wiita, P.J. 1987, MNRAS, 226, 531
 _____. 1991, ApJ, 373, 325

Hutchings, J.B., Price, R., & Gower, A.C. 1988, ApJ, 329, 122

Jaffe, W., Ford, H., Ferrarese, L., van den Bosch, F., & O'Connell, R.W.O. 1993, Nature, 364, 213

Kapahi, V.K. 1990, in Parsec-Scale Radio Jets, eds. J.A. Zensus, & T.J. Pearson (Cambridge, Cambridge Univ. Press) 304

Kapahi, V.K., Athreya, R.M., Subrahmanya, C.R., Hunstead, R.W., Baker, J.C., McCarthy, P.J., & van Breugel, W. 1995, J. Astrophys. Astr. Supp., 16, 125

Königl, A., & Kartje, J. 1994, ApJ, 434, 446

Laing, R.A., Jenkins, C.R., Wall, J.V., & Unger, S.W. 1994 in The Physics of Active Galaxies (ASP Conf. Ser. 54), eds. G.V. Bicknell, M.A. Dopita, & P.J. Quinn (San Francisco, ASP), 201

Laing, R.A., Riley, J.M., & Longair, M.S. 1983, MNRAS, 204, 151

Lawrence, A. 1991, MNRAS, 252, 586

Liu, R., Pooley, G., & Riley, J.M. 1992, MNRAS, 257, 545

Netzer, H., & Laor, A. 1993, ApJ, 404, L51

Padovani, P., & Urry, C.M. 1992, ApJ, 387, 449

Rawlings, S., & Saunders, R. 1991, Nature, 349, 138

Readhead, A.C.S. 1995, Proc. Nat. Acad. Sci., 92, 11447

Rees, M.J. 1994, QJRAS, 35, 391

Saikia, D.J., & Kulkarni, V.K. 1994, MNRAS, 270, 897

Scheuer, P.A.G. 1974, MNRAS, 166, 513

_____. MNRAS, 277, 331

Siah, M.J., & Wiita, P.J. 1990, ApJ, 363, 411

Singal, A.K. 1993a, MNRAS, 262, L27

_____. 1993b, MNRAS, 263, 139

_____. 1995, Proc. Nat. Acad. Sci., 92, 11407

_____. 1996, MNRAS, 278, 1069

Urry, C.M., & Padovani, P. 1995, PASP, 107, 803

Wiita, P.J., & Gopal-Krishna. 1990, ApJ, 353, 476

Yi, I., Field, G.B., & Blackman, E.G. 1994, ApJ, 432, L31

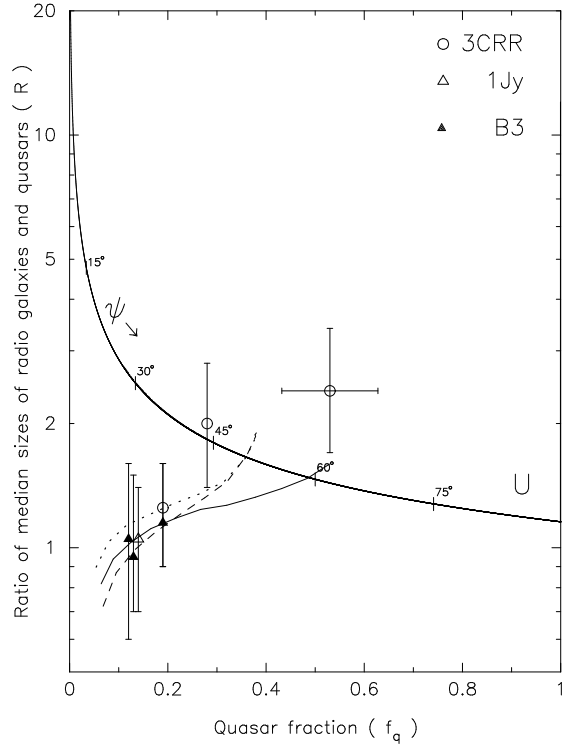


Fig. 1.— A plot of R versus f_q for the subsets of three flux-limited samples selected at meter-wavelengths. The data shown with error bars are reproduced from Singal (1995). The thin curve “U” depicts the prediction of the unified scheme for such orientation bias-free samples, over a range in the torus half-angle ψ . The three other curves represent our predictions of the unified scheme incorporating temporal evolution, as described in the text. Each of the curves covers a two orders-of-magnitude range in radio luminosity, increasing to the right. The input parameters $(\Gamma, a, b_1, \psi_{max})$ are $(1.8, 0.38, 0.18, 1.1 \text{ rad})$ for the solid curve, $(1.8, 0.40, 0.25, 0.9 \text{ rad})$ for the dashed curve, and $(2.0, 0.40, 0.30, 0.9 \text{ rad})$ for the dotted curve. The other input parameters were set (following the empirical results mentioned in the text) to: $b_2 = 0.8$ and $\psi_{min} = 0.2 \text{ rad}$. Note that a horizontal error bar is also shown for the rightmost data point; it represents a typical 1σ error of these 3CRR data points, each of which is based on a relatively small set of sources.